Closed loop optimization of quasi-inhomogeneous optical coatings

Henrik Fabricius

Lys & Optik, Danish Academy of Technical Sciences
Hjortekaersvej 99, DK-2800 Lyngby, Denmark

ABSTRACT

Errors inherent to the approximateness and incompleteness of the inverse Fourier transformation technique can be partly compensated by using successive approximations. Especially interesting is the situation where it is possible to optimize the primary approximate solution efficiently by means of repeated iterations on unchanged conditions (closed loop optimizations). It is shown that the degree of convergence of the closed loop optimization process and the obtainable result depend on the actual choice of Q-function. The results are similar when the closed loop optimizations are performed prior to and after conversion into a two-indexed quasi-inhomogeneous solution employing double layer equivalents. The subject of the optimization of the number of layers in the two-index solution is discussed and a couple of new Q-functions that are better suited for closed loop optimizations of both converted and unconverted coatings than some of the best known existing Q-functions are presented.

1. INTRODUCTION

The author is particularly interested in the design and production of quasi-inhomogeneous coatings with a smooth and precise performance in a broad spectral range. Typical examples could be tristimulus-filters for colour measurements[1], Y-filters for light measurements, linearization filters for CCD based spectrometer-systems[1] with a limited dynamic range, and filters for by routine calibrations of e.g. vision systems.

It is well-known that the inverse Fourier transform technique is suited for the design of the desired type of coatings.[1,2,3,4] However, it is also well-known that the technique suffers from different incompletenesses and that it builds on approximate analytical relations.[1,2,5,6,7,8,9,10] In future all problems may be solved analytically. This is, however, far from reality today. Not only do we miss proper definitions of the spectral amplitude and phase-functions Q(k) and $\Phi(k)$, we may also need to employ different initial correction techniques[1,10] and conversion-techniques[10] as well as numerical optimization techniques[1,2,6,7] to be able to design a coating that has the desired properties when produced.[10]

A proper definition of the spectral function Q(k) is essential. But the best choice is not necessarily the one which gives the closest fit after the first inverse Fourier transformation. When doing closed loop optimizations, the most important thing is that the calculation converges towards the best possible solution.

The author experienced that closed loop optimizations tend to decrease the relative deviation between the desired and the obtained spectral curves on the cost of the absolute deviation when employing different well-known Q-functions.[5,6,7,8,11] This is a problem, because we are often just as concerned with the absolute deviation between the desired and obtained filter-curves as with the relative deviation.

The purpose of this paper is to present a couple of new Q-functions that are better suited for closed loop optimizations of both converted and unconverted coatings. The conversion technique used is based on the application of double layer equivalents (DLE).[10,11] It implies that the continuous optical admittance profile is divided into N relatively thin layer-elements prior to the conversion. The conversion is only approximate, and the deviations increase with the relative optical thickness of the unconverted layers. However, it appears that it is possible to convert layer-elements of an unexpected large optical thickness, when the layer-elements are converted alternately into HL-equivalents and LH-equivalents. It is shown that two-index solutions composed of relative thick layer-elements still are suited for closed loop optimizations, and that it is possible to reduce errors inherent to a number of approximations introduced in a realistic design process by closed loop optimizations.

2. BASIC THEORY

The Fourier transform technique described here is based on the original works of Sossi and Kard.[2,12,13] They showed that it is possible to relate the spectral transmittance of an inhomogeneous non-absorbing layer to its refractive index profile n(x)

0-8194-1305-4/93/$6.00

by the approximate expression

$$\int_{-\infty}^{\infty} \frac{dn}{dx} \frac{1}{2n} \exp(ikx)\, dx = Q(k) \exp[i\Phi(k)] \tag{1}$$

where Q(k) is a suitable even function of the desired transmittance T(k), $\Phi(k)$ is a phase function that must be an odd function to ensure that n(x) is real, x is twice the optical distance from the centre of the inhomogeneous layer, n(x) is the refractive index and k the wave number $2\pi/\lambda$.

Eq. (1) can be generalized to include the case of non-normal incidence by replacing the refractive index n(x) by the corresponding optical admittance $\eta(x)$ and by introducing the following expression for x

$$x = 2 \int_0^z n(u) \cos\Theta_p \, du \tag{2}$$

where Θ_p is the angle of propagation in the medium of index n(x), and where z is the geometrical coordinate within the layer. Applying a Fourier transformation to Eq. (1) and integrating with respect to x we have

$$\eta(x) = \eta_o \exp\left(\frac{2}{\pi} \int_0^{\infty} \frac{Q(k)}{k} \sin[\Phi(k) - kx]\, dk \right) \tag{3}$$

With $\eta(x)$ expressed in discrete numbers, we evaluate the corresponding spectral performance, using conventional matrix multiplications[14] and assuming each layer element to be homogeneous.[3,6,10]

The optical admittance modulations tend to extend beyond the permitted optical admittance range when designing filters which possess a high reflection in different parts of the spectrum.[1,8] As reported previously[1], we still find that the best way to reduce the modulation of the optical admittance profile is to introduce the following phase function

$$\Phi(k) = \frac{\pi k}{k_{min} + k_{max}} - 2 \sin\left(N\pi \frac{k - k_{min}}{k_{max} - k_{min}} \right) \tag{4}$$

where N is a real number that is typically in the 1 - 5 range; k_{min} and k_{max} are spectrally limiting wave numbers.

3. THE Q-FUNCTION

A proper definition of the spectral function Q(k) is essential. In the course of time a number of approximate Q-functions have been presented which vary in accuracy.[5,6,7,8,15] Sossi introduced the following expression, which was also used by Dobrowolski and Lowe.[2,3]

$$Q_1(k) = (1/2[1/T(k) - T(k)])^{1/2} \tag{5}$$

However, this expression does not work well at high reflectance, and it is not considered further in this work. Bovard derived some better expressions[5,6,15]

$$Q_2(k) = (- \ln[T(k)])^{1/2} \tag{6}$$

$$Q_3(k) = \text{Arctgh}([1 - T(k)]^{1/2}) \tag{7}$$

The author experienced that the application of the Q_2-function tends to deliver refractive index profiles with too small index-modulation whereas the opposite is the case when the Q_3-function is applied.

3.1 Iterative determination of Q(k) (closed loop optimization)

Despite the approximate nature of the Q-functions, it is possible to obtain acceptable designs by changing Q(k) iteratively by means of successive approximations as explained by several workers.[1,2,6,7] It was Sossi's idea[2] to substitute back the

obtained transmission curve into the Q(k) calculation and to add the difference between these intermediate Q-values, $Q_a(k)$, and the original Q-values, $Q_0(k)$, to the latest Q-values, $Q(k)_{j-1}$, to obtain a new and hopefully improved set of Q-values, $Q(k)_j$, as expressed by

$$Q(k)_j = Q(k)_{j-1} + [Q_0(k) - Q_a(k)] \tag{8}$$

The j index indicates the number of executed calculation turns when the operation is repeated several times. Especially interesting is the situation where it is possible efficiently to reoptimize the primary approximate solution by means of closed loop optimizations (repeated iterations on unchanged conditions). The convergence properties of the closed loop optimization process depends on a proper definition of the approximate Q-function as well as on the approximations relation.

The relative close relation that has been observed between $Q^2(k)$ and the logarithmic function made the author consider a slightly different iteration technique

$$Q(k)_j = \{ Q^2(k)_{j-1} + [Q_o^2(k) - Q_a^2(k)] \}^{1/2} \tag{9}$$

It appears that the speed of convergence drops with a factor of about 2 when this equation is applied instead of the original. However, the improvements of the designs that may be achieved are nearly identical, and there is no clear tendency that one relation should be better than the other in terms of the quality of the designs obtained.

More interesting is that we are to see that the obtainable results clearly depend on the actual choice of Q-function. However, we will derive a couple of new Q-functions at first.

3.2 The narrow-banded reflection related Q-function.

Imagine that we want to design a narrow-banded single reflectance filter with a half-width of Δk and maximum reflection at the wave number k_1 (normal incidence). In this case, the following relation can be derived from Eq.(1)

$$\frac{n'(x)}{n(x)} = 4Q(k_1) \frac{\sin(x\Delta k/2)}{\pi x} \cos k_1 x \tag{10}$$

Assuming a sufficient narrow-banded reflection ($\Delta \ll k_1$) the following equation appears that describes the refractive index profile

$$n(x) = n_a \exp\left(\frac{2\Delta k}{\pi} \frac{Q(k_1)}{k_1} \sin k_1 x \right) \approx n_a + \frac{2n_a \Delta k}{\pi} \frac{Q(k_1)}{k_1} \sin k_1 x \tag{11}$$

This equation obviously describes a rugate structure with an average index n_a and an index modulation n_p of

$$n_p = \frac{4n_a \Delta k}{\pi} \frac{Q(k_1)}{k_1} \tag{12}$$

According to ref.[1], we have the following alternative expression for n_p

$$n_p = \frac{4n_a Q_3(k_1)}{k_1 OT_{tot}} \tag{13}$$

where OT_{tot} is the total optical thickness of the coating and where $Q_3(k_1)$ is expressed by Eq. (7).

By comparison of Eqs. (12) and (13) the following expression appears

$$Q(k_1) = \frac{\pi Q_3(k_1)}{OT_{tot} \Delta k} \tag{14}$$

It is also possible to estimate an expression for Δk on the basis of the relations in refs. [1, 16]. The approximate width

of the range of maximum reflection is

$$\Delta k_b = n_p k_1/(2n_a) = 2Q_3(k_1)/OT_{tot} \tag{15}$$

and the difference in wave numbers between the two closest points around the central dip where the rugate is fully transmitting is

$$\Delta k_f = 2\pi/OT_{tot}\,(1 + [Q_3(k_1)/\pi]^2)^{1/2} \tag{16}$$

leading to the approximate expression for the half-width Δk

$$\Delta k \approx (\Delta k_b + \Delta k_f) = \pi/OT_{tot}(Q_3(k_1)/\pi + (1 + [Q_3(k_1)/\pi]^2)^{1/2}) \tag{17}$$

The resultant Q-function

$$Q_4(k) = Q_3(k)/(Q_3(k)/\pi + (1 + [Q_3(k)/\pi]^2)^{1/2}) \tag{18}$$

fulfils the essential requirements that

$$Q(k) = 0 \qquad \text{for } T(k) = 1 \tag{19}$$

and

$$\frac{dQ^2(k)}{dT(k)} = -1 \quad \text{for } T(k) = 1 \tag{20}$$

that was mentioned in ref. [7].
This does also apply for the following Q-function which is considered

$$Q_5(k) = Q_3(k)/(1 + [Q_3(k)/\pi]^2)^{1/2} \tag{21}$$

4. CLOSED LOOP OPTIMIZATION

In the following we test the functioning of the four Q-functions $Q_2(k)$, $Q_3(k)$, $Q_4(k)$ and $Q_5(k)$ in a closed loop optimization process. In each case, we try to closed loop optimize a coating by doing repeated iterations on the Q-function leaving the conditions unchanged. The overall performance of the coating is expressed by means of two merit-values plotted for the first one hundred calculation turns.

The merit function M-abs is a measure of the average absolute deviation between the transmission values of the desired and the present spectral curves in a selected range of wave numbers k_j to k_m

$$\text{M-abs} = \left(\frac{1}{N_m} \sum_{i=j}^{m} \Delta T^2(k_i) \right)^{1/2} \qquad (N_m = m - j + 1) \tag{22}$$

whereas the merit function M-rel is a measure of the corresponding relative deviation

$$\text{M-rel} = \left(\frac{1}{N_m} \sum_{i=j}^{m} \frac{\Delta T^2(k_i)}{T^2(k_i)} \right)^{1/2} \tag{23}$$

4.1 The Gaussian shaped reflection filter

The first filter we want to design is a Gaussian shaped reflection filter. This type of filter was selected for the first test of the calculations for the following reasons: The characteristic shows both low and high reflection[7] (R_{max} = 99%), but the transition between high transmission and high reflection is smooth in such a way that the initial corrections applied in ref. [1] are not necessary. Furthermore, it is possible to keep the refractive index profile within a reasonable refractive index range, although, we intend to achieve a peak-reflection of 99%.

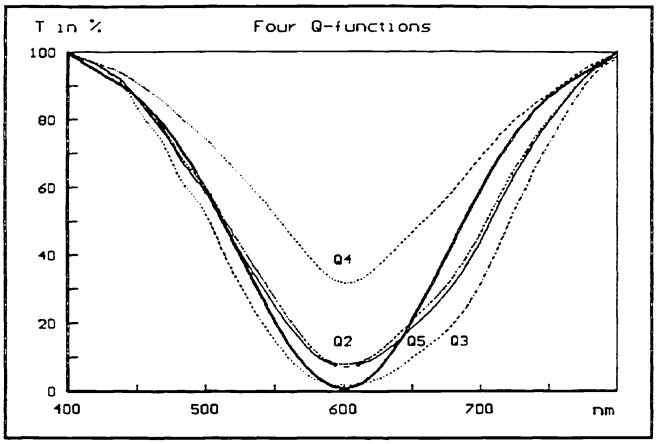

Figure 1. Bold curve is the Gaussian shaped rejection filter we want to design. The remaining 4 curves are the transmission curves obtained as the result of the first inverse Fourier transformation when the different Q-functions are applied. The total optical thickness of the coating is set to be 7μm.

The bold curve in figure 1 shows the transmission curve of the Gaussian shaped rejection filter we want to design. The remaining 4 curves are the transmission curves obtained as the results of the first inverse Fourier transformation when the different Q-functions are applied. We note that the peak reflection is nearly obtained by means of the Q_3-function whereas this is far from the case when the new Q_4-function is applied. Furthermore, we note that the second-largest peak reflection is obtained by means of the new Q_5-function lying slightly underneath the Q_2-curve. It is obvious that none of the results obtained by now are satisfactory. In the following we discuss the situation where the curves are closed loop optimized by means of successive approximations on the fixed conditions that: it is assumed that the refractive index profile passes continuously into the boundary media and that the thin-film materials are non-dispersive; the angle of incidence is normal; the total optical thickness of the coating is 7μm; the refractive index modulations are reduced by means of the phase function in Eq. (4) (N = 2.2); the number of k-values is 200 and the number of x-values is 100.

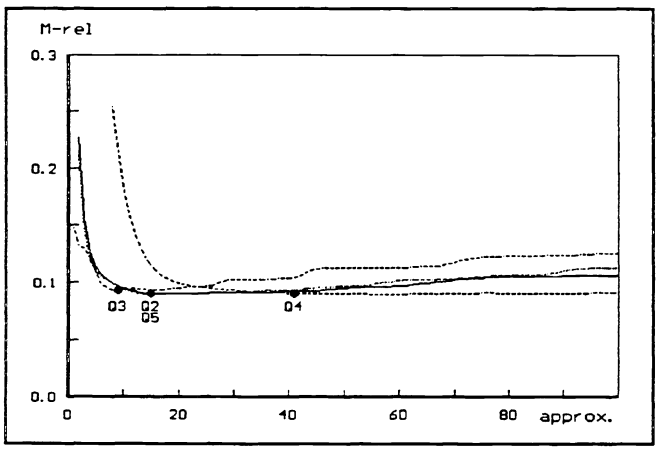

Figure 2. Plot of the merit-value M-rel as function of the executed number of calculation turns in case of the design of the Gaussian shaped rejection filter in fig. 1

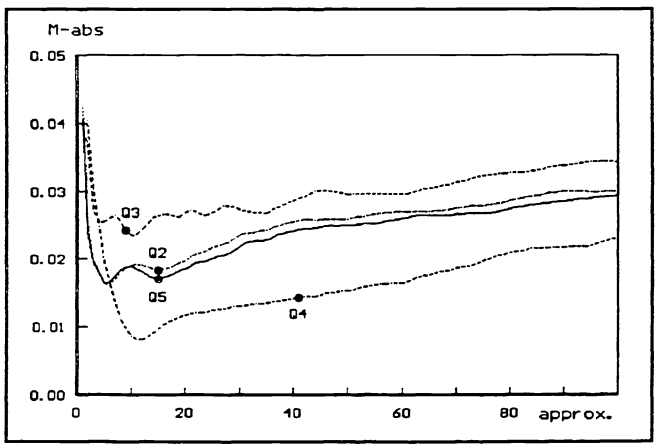

Figure 3. Plot of the merit value M-abs as function of the executed number of calculation turns in case of the design of the Gaussian shaped rejection filter in fig. 1.

Figures 2 and 3 are plots of the two merit values M-rel and M-abs, as function of the executed number of iteration when

performed on the four Q-functions, Q_2, Q_3, Q_4 and Q_5. It is seen from the figures that both the relative and the absolute deviations decrease rapidly at the beginning of the iterations. However, from some point the decrease in the relative deviation happens on the expense of the absolute deviation, and finally both types of deviations increase again. It is obvious that none of the calculations really converge. In each case the relative deviation decreases towards approximately the same minimum value as marked by the black spots in figure 2 (0.090 for Q2, Q4 and Q5 and 0.093 for Q3). However, as seen from figure 3, the absolute deviations are quite different at the same positions. The best result is clearly obtained by means of the new Q_4-function whereas the worst result is obtained by means of the Q_3-function. The second-best result is obtained by means of the Q_5-function, although, it functions quite similar to the Q_2-function. Figure 4 shows the transmission-curve that was obtained by means of the new Q_4-function at the marked position (41 iterations) and figure 5 shows the corresponding refractive index profile.

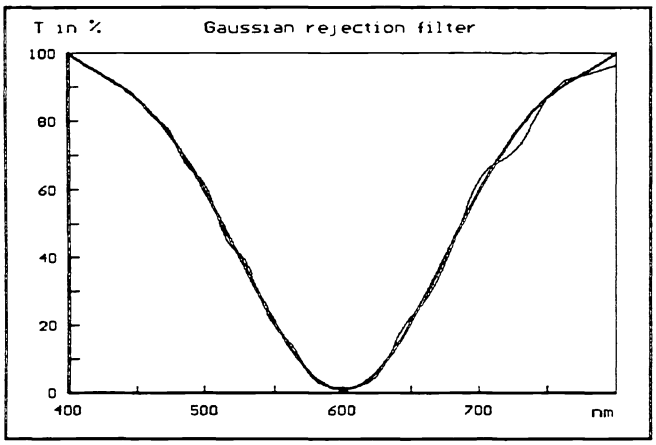

Figure 4. Transmission curve that is obtained by means of the new Q_4-function after 41 iterations (see figure 2).

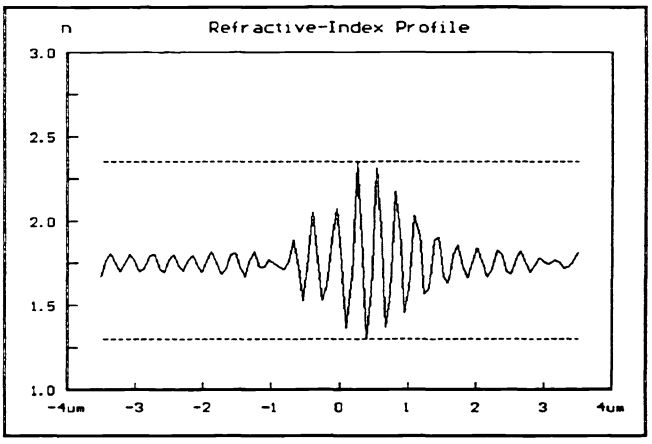

Figure 5. Refractive index profile corresponding to the transmission curve in figure 4. The total optical thickness is 7μm.

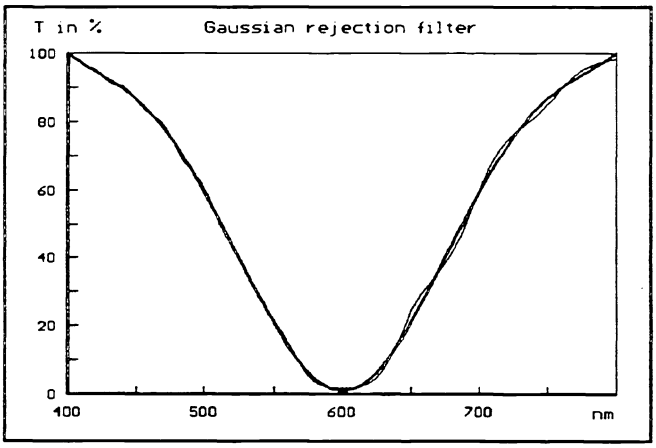

Figure 6. Transmission curve obtained by means of the new Q_4-function after 17 iterations. The bold curve is the desired curve and the plain curve is the obtained curve.

The number of iterations it takes to reach the optimum depends on the choice of Q-function. A larger number of iterations is of course of disadvantage as to the computing time. However, this is actually only of little importance as far, as each calculation turn did only take about 25 seconds on a Compac 386/20 deskpro computer.

The final choice of filter-design does of course depend on how the designer weight the importance of the absolute deviations to the relative deviations. In this respect a slower convergence of the calculations may be considered an advantage. Figure 6 shows the transmission curve obtained after 17 iterations. This curve is obviously smoother than the curve in figure 4.

5. Closed loop optimization of two-index solutions

In practice the refinement by means of the successive approximations includes a compensation of all different types of minor approximations introduced in the calculations[2]. This makes the successive approximation technique a very efficient tool in

a realistic design-situation where the conditions differ more or less from the presumptions that were made when the basic relations were derived. Typical problems could be: the inclusion of standard substrates[1], the limited optical thickness of real thin films[1,2], the limited range of refractive indices of real thin film materials[8], incidence of non-perfectly collimated and non-polarized light, and the dispersion of the refractive index of real thin film materials[10].

5.1. Conversion into two-index solution

The application of Eq.(3) implies that the thin film is non-dispersive. However, this is normally not the case[10], and especially not at low wavelength. In a previous paper the author showed that it is possible to take the dispersion of the refractive index of real thin film materials into account when the continuous optical admittance profile is converted into a quasi-inhomogeneous two-index solution and reoptimized by means of closed loop optimizations prior to the production.[10]

The conversion technique[10] is easily modified to include the case of non-normal incidence of light, and it appears to be possible to design coatings that can be applied for non-polarized light at angles of incidence of up to +- 20° by specifying the state of polarization to be S in the Fourier calculations and by subsequently reoptimizing the coating to fit for non-polarized light by means of closed loop optimizations. A practical feature of the developed technique of conversion is that the continuous optical admittance profile is converted into the actual layer-system we have to deposit at normal incidence.

However, the main reason why we perform a conversion of the continuous admittance profile prior to the production is of course that we have developed a proprietary process steering system that makes it possible to produce the coatings designed by means of conventional vacuum-techniques.

5.2 Optimization of the number of layers in the two-index solution

The conversion technique that is based on the application of double layer equivalents implies that the continuous optical admittance profile is divided into N relatively thin layer-elements prior to the conversion. In practice these layer-elements are equivalent to the N sampling elements of the continuous optical admittance profile used for the calculation of the transmission curve. Consequently, the criterion for the conversion is a sampling-criterion as expressed by

$$OT = OT_{tot}/N = n_p t_p \cos\Theta_p \ll \lambda \tag{24}$$

that origins from the first order approximations performed onto the sine and cosine functions in refs. [10] and [11]

$$\mathbf{M}_p = \begin{bmatrix} \cos\Phi_p & i\sin\Phi_p/\eta_p \\ i\eta_p\sin\Phi_p & \cos\Phi_p \end{bmatrix} \approx \begin{bmatrix} 1 & i\Phi_p/\eta_p \\ i\eta_p\Phi_p & 1 \end{bmatrix} \tag{25}$$

In the following we name the characteristic matrix of the unconverted layer $\mathbf{M}_p$' and the characteristic matrix of the double layer equivalent by $\mathbf{M}_p$.

It is obvious that the conversion is only approximate and that the deviations increase with the relative optical thickness of the unconverted layers. However, the conversion technique is preferential to the conventional Herpin conversion technique[16,17] in the respect that it is single stepped and suited for fast closed loop optimizations of the approximate two-indexed solution.[10]

It is of interest to investigate what happens when the optical thickness of the layer-elements is enhanced prior to the conversion. Relaxing the demand of Eq. (24) the zero-order approximation of $\cos(\Phi_p)$ soon becomes too inexact. The exact expressions corresponding to the matrix-elements of a HL-double layer equivalent are:

$$\mathbf{M}_{p11} = \cos\Phi_{pH}\cos\Phi_{pL} - (\eta_L/\eta_H)\sin\Phi_{pH}\sin\Phi_{pL} \tag{26}$$

$$\mathbf{M}_{p12} = \cos\Phi_{pH}\sin\Phi_{pL}/\eta_L + \cos\Phi_{pL}\sin\Phi_{pH}/\eta_H \tag{27}$$

$$\mathbf{M}_{p21} = \eta_L\cos\Phi_{pH}\sin\Phi_{pL} + \eta_H\cos\Phi_{pL}\sin\Phi_{pH} \tag{28}$$

$$\mathbf{M}_{p22} = \cos\Phi_{pH}\cos\Phi_{pL} - (\eta_H/\eta_L)\sin\Phi_{pH}\sin\Phi_{pL} \tag{29}$$

It appears that the expressions for M_{p11} and M_{p22} differ. Furthermore they interchange in case of a LH-double layer conversion.

The relative deviations between the matrix-elements of the characteristic matrix of the equivalent, M_p, and the unconverted layer, M_p', were calculated as function of the refractive index of the un-converted layer, n_p, in the case of normal incidence of light, $n_H = 2.35$, $n_L = 1.3$ and $OT/\lambda = 0.05$. Figure 7 is a graphical illustration of the results obtained. The dotted curve belongs to M_{p12}, the dashed curve to M_{p21} and the solid curves to M_{p11} and M_{p22}. The uppermost curve belongs to M_{p11} in case of a HL-equivalent. Otherwise it belongs to M_{p22}. In figure 8 the relative deviations have been plotted as function of the relative optical thickness of the un-converted layer, OT/λ, in case of normal incidence of light, $n_H = 2.35$, $n_L = 1.3$ and $n_p = 1.8$.

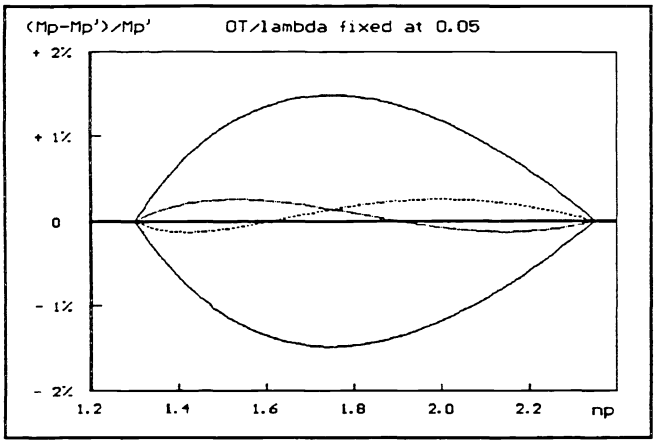

Figure 7. The relative deviations between the matrix elements of the characteristic matrix of the double layer equivalent, M_p, and the unconverted layer, M_p', as function of the refractive index of the un-converted layer, n_p, in the case of normal incidence of light, $n_H = 2.35$, $n_L = 1.3$ and $OT/\lambda = 0.05$. (M_{p11} and M_{p22} ---, M_{p12} ..., M_{p21} —).

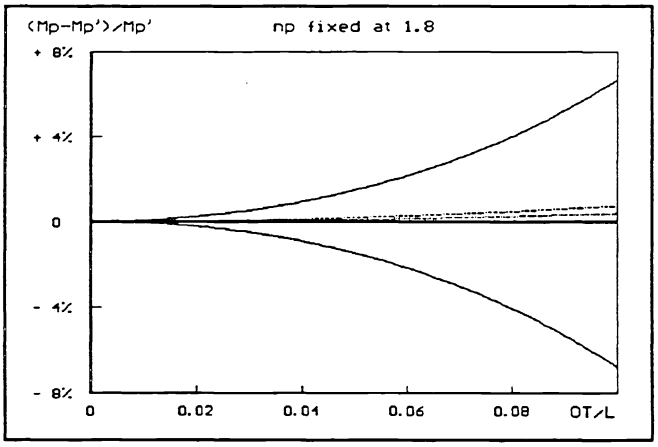

Figure 8. The relative deviations between the matrix elements of the characteristic matrix of the double layer equivalent, M_p, and the unconverted layer, M_p', as function of the relative optical thickness of the un-converted layer, OT/λ, in case of normal incidence of light, $n_H=2.35$, $n_L=1.3$ and $n_p = 1.8$. (M_{p11} and M_{p22} ---, M_{p12} ..., M_{p21} —).

When the optical thickness of the unconverted layer is enhanced the largest deviations obviously occur within M_{p11} and M_{p22} and at medium values of n_p. Furthermore it appears that these deviations are of equal amount but opposite sign.

Labelling the relative deviation of M_{p11} by α

$$0 \leq \alpha \ll 1 \tag{30}$$

and the matrix-elements of M_p' by A, B, C and A, this may be expressed as

$$M_{pHL} \approx \begin{bmatrix} (1+\alpha)A & iB \\ iC & (1-\alpha)A \end{bmatrix} \tag{31}$$

$$M_{pLH} \approx \begin{bmatrix} (1-\alpha)A & iB \\ iC & (1+\alpha)A \end{bmatrix} \qquad (32)$$

When comparing Eqs. (31) and (32) and taking into account the influence of the matrix-element of the overall system-matrix on the obtained transmission-curve, it is obvious that the influence of the deviations may be reduced by converting the layer-elements alternately into HL-equivalents and LH-equivalents. Furthermore, this reduces the total number of layers in the approximate two-index solution to be (N + 1), which should be compared to the total number of layers in a conventional Herpin conversion which is somewhere between (2N + 1) and 3N.[16,17]

The optimal number of layers in the two-index solution is experienced to be approximately four times the number of cycles on the optical admittance profile. A considerably larger number of layers is not experienced to be of advantage. At to low numbers strong reflections occur at the low-wavelength range.

5.3 The modified Y-filter for slightly non-normal incidence.

The second filter we want to design is a modified Y-filter for CIE colour measurements (see figure 9). This time we are going to try the closed loop optimizations on a realistic design-situation where the conditions are much more complicated than in the first example where we designed the Gaussian rejection filter.

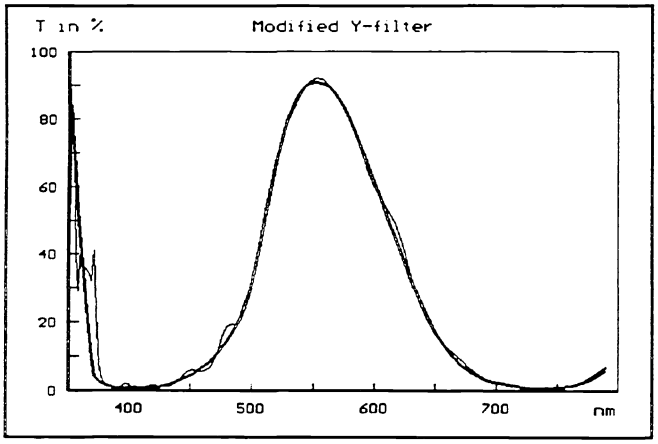

Figure 9. Bold curve shows the desired modified Y-filter. The plain curve shows the transmission curve that was obtained by means of the new Q_4-function after 66 iterations.

This time the conditions are as follows: it is assumed that the filter should be applied for an angle of incidence of 6 degrees and non-polarized light; the thin film materials are ZnS and Misch Fluoride[10] and the dispersion of the materials is taken into account as explained in ref. [10]; the total optical thickness of the filter is 5μm and the limited optical thickness of the filter is taken into account by doing corrections on the characteristics as explained in ref. 1. The optical admittance modulations are reduced by application of the phase function in Eq. (4) (N = 2.2); the optical admittance profile is truncated to the boundaries of the permitted range[8] when extending beyond them (the optical thickness of each layer element is left unchanged); the filter is deposited onto a BK7 glass substrate and cemented with a cover glass and the missing adaptation to the boundary media is compensated by overlaying quintic matching layers as explained in ref. 1; the number of k-values is 100 and the number of x-values is 80, which is approximately 4 times the number of cycles on the optical admittance profile; the optical admittance profile is converted into a two-index solution by means of the developed conversion technique and the whole thing is closed loop optimized by means of successive approximations. The Merit-calculations cover the wavelength range from 400nm to 750nm (see ref. 10 for comments on the wavelength range below 400nm).

The figures 10 and 11 are plots of the two merit values, M-rel and M-abs, as function of the executed number of iterations when performed on the four Q-functions, Q_2, Q_3, Q_4 and Q_5. When compared to the figures 3 and 4, it appears that the tendencies are once again the same. It is apparent that none of the calculations really converge. Both the relative and the absolute deviations decrease rapidly at the beginning of the iterations but suddenly an optimum is reached (marked by dark spots). Once again the relative deviation decreases to approximately the same limit in case of the 3 Q-functions Q_2, Q_4 and Q_5 ($\approx$ 0.224) whereas the result is worse in case of the Q_3-function (0.251). And according to figure 11, the absolute deviations are again quite different at the same positions. The best result is definitely obtained by means of the new Q_4-function whereas the worst result is obtained by means of the Q_3-function. The second-best result is obtained by means of the Q_5-function, although, it functions quite similar to the Q_2-function. The plain curve in figure 9 shows the transmission-curve obtained by means of the new Q_4-function at the marked position (66 iterations). Figure 12 shows the corresponding optical admittance profile and figure 13 is the two-indexed conversion of this profile.

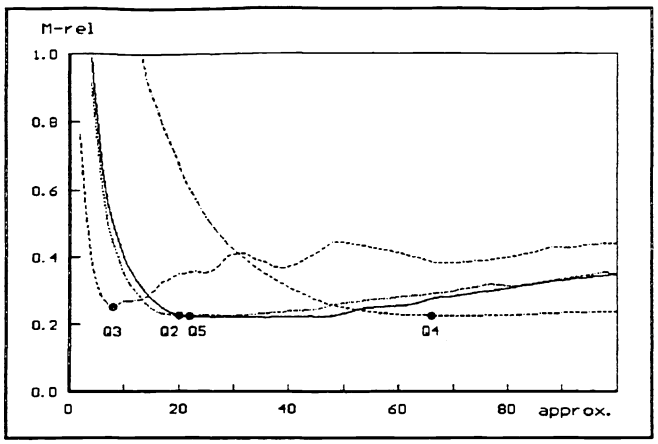

Figure 10. Plot of the merit-value M-rel as function of the executed number of calculation turns in case of the design of the modified Y-filter in figure 9.

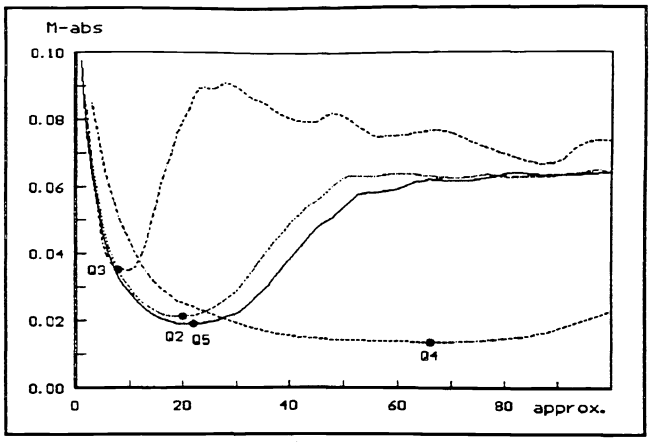

Figure 11. Plot of the merit value M-abs as function of the executed number of calculation turns in case of the design of the modified Y-filter in figure 9.

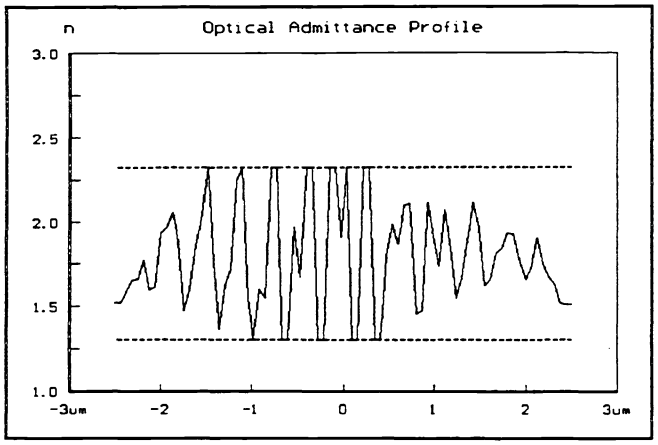

Figure 12. The optical admittance profile corresponding to the optimized transmission curve in figure 9.

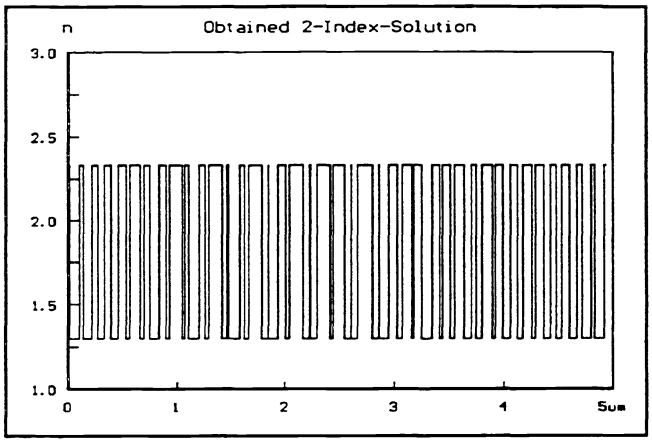

Figure 13. Two index convert of the optical admittance profile in fig. 12. The number of layers is 81.

6. DISCUSSION

It is interesting to note the close mathematical relationship between the new Q_4 and Q_5-functions and the old Q_3-function. The difference between them is the bandwidth estimate used in the denominator in Q_4 and Q_5. Maybe an even better Q-expression may be obtained by choosing the right expression for the bandwidth.

It is also interesting to note the close functional relation between the new Q_5-function and the old Q_2-function.

7. CONCLUSIONS

It was shown that it is possible to compensate for a number of errors inherent to the inverse Fourier transformation technique by changing the Q-function iteratively. However, the obtainable result obviously depends on the definition of the Q-function.

Two new Q-functions were derived and it was shown that they perform better in a closed loop optimization process than some of the most well-known Q-functions.

The results are similar when the closed loop optimizations are performed prior to and after the conversion into a quasi-inhomogeneous conversion employing double layer equivalents.

The optimization of the number of layers in the two-indexed solution was discussed, and it was shown that it is possible

to convert unexpected thick layer elements with the developed technique.
Finally, it was demonstrated that it is possible to take into account slightly non-normal incidence of non-polarized light.

8. REFERENCES

1. Henrik Fabricius, "Gradient Index Filters : Designing filters with steep skirts, high reflection, and quintic matching layers," Applied Optics, **31** (no. 25), pp. 5191 - 5196 (Sept. 1992)

2. L. Sossi, "A method for the synthesis of multilayer dielectric interference coatings," Eesti NSV Tead. Akad. Toim. Fuus. Mat. **23**, pp. 229 - 237 (1974). An English translation of this paper is available from the Translation Services of the Canada Institute for Scientific and Technical Information, National Research Council, Ottawa, Ontario, Canada K1A OS2.

3. J. A. Dobrowolski and D. Lowe, "Optical Thin Film Synthesis Program Based on the Use of Fourier Transforms," Applied Optics **17** (no. 19), pp. 3039 - 3050 (Oct. 1978).

4. J. A. Dobrowolski, "Comparison of the Fourier transform and flip-flop thin-film synthesis methods," Applied Optics, **25** (no. 12), pp. 1966 - 1972 (June 1986).

5. B. G. Bovard, "Derivation of a matrix describing a rugate dielectric thin film," Applied Optics, **27** (no. 10), pp. 1998 - 2005 (May 1988)

6. B. G. Bovard, "Rugate filter design : the modified Fourier transform technique," Applied Optics, **29** (no. 1), pp. 24 - 30 (Jan. 1990).

7. P. G. Verly and J. A. Dobrowolski, "Synthesis of high rejection filters with the Fourier transform method," Applied Optics, **28** (no. 14), pp. 2864 - 2875 (July 1990)

8. P. G. Verly and J. A. Dobrowolski, "Iterative correction process for optical thin film synthesis with the Fourier transform method," Applied Optics, **29** (no. 25), pp. 3672 - 3684 (Sept. 1990)

9. P. G. Verly, J. A. Dobrowolski and R. R. Willey, "Fourier-transform method for the design of wideband antireflection coatings," Applied Optics, **31** (no. 19), pp. 3836 - 3846 (July 1992)

10. Henrik Fabricius, "Gradient Index Filters : conversion into a two-index solution by taking into account dispersion," Applied Optics, **31** (no. 25), pp. 5216 - 5220 (Sept. 1992).

11. W. T. Southwell, "Coating design using very thin high- and low-index layers," Applied Optics, **24** (no. 4), pp. 457 - 460 (Feb. 1985).

12. L. Sossi and P. Kard, " On the theory of the reflection and transmission of light by a thin inhomogeneous dielectric film," Eesti NSV Tead. Akad. Toim. Fuus. Mat. **17**, pp. 41 - 48 (1968). An English translation is available, see Ref. 2.

13. L. Sossi, "On the theory of the synthesis of multilayer dielectric light filters," Eesti NSV Tead. Akad. Toim. Fuus. Mat. **25**, pp. 171 - 176 (1976). An English translation is available, see Ref. 2.

14. H. A. Macleod, Thin-Film Optical Filters, 2nd ed. (Adam Hilger Ltd., Bristol, 1986), Chap. 2, p. 11 - 48.

15. B. G. Bovard, "Fourier transform technique applied to quarterwave optical coatings," Applied Optics, **27** (no. 15), pp. 3062 - 3063 (Aug. 1988)

16. W. H. Southwell, "Spectral response calculations of rugate filters using coupled-wave theory'" J. Opt. Soc. Am. A., **5** (no. 9), pp. 1558 - 1564 (Sept. 1988)

17. J. A. Dobrowolski and S. H. C. Piotrowski, "Refractive index as a variable in the numerical design of optical thin film systems," Applied Optics, **21** (no. 8), pp. 1502 - 1511 (April 1982).

18. T. Skettrup, "Three layers approximation of dielectric thin film systems," Applied Optics, **28**, pp. 2860 - 2863 (1989)